

## Evidence of 3D and 2D electron transport in amorphous Cu-Ti films

This article has been downloaded from IOPscience. Please scroll down to see the full text article.

1991 J. Phys.: Condens. Matter 3 2937

(<http://iopscience.iop.org/0953-8984/3/17/010>)

View [the table of contents for this issue](#), or go to the [journal homepage](#) for more

Download details:

IP Address: 171.66.16.147

The article was downloaded on 11/05/2010 at 12:04

Please note that [terms and conditions apply](#).

# Evidence of 3D and 2D electron transport in amorphous Cu–Ti films

C Shearwood† and D Greig

Department of Physics, University of Leeds, Leeds LS2 9JT, UK

Received 18 July 1990, in final form 2 January 1991

**Abstract.** Measurements are presented of the temperature and magnetic field dependences of the electrical resistivity of sputtered amorphous Cu–Ti films in a series of experiments designed to examine possible changes over four decades of thickness. The resistivity of all the films was found to be approximately  $230 \mu\Omega \text{ cm}$ , and this, together with selected TEM micrographs, confirmed that the specimens were amorphous, crack-free and homogeneous. The experiments show quite clearly the transition from three-dimensional to two-dimensional behaviour as predicted by models of quantum interference.

## 1. Introduction

Although the influence of quantum corrections to the transport properties of archetypal amorphous alloys such as Cu–Ti have been widely studied, relatively few measurements have been made on thin films, and in particular the differences in form of the temperature and magnetic field dependences in 3D-to-2D specimens of a particular disordered alloy have never been investigated. The measurements presented in this paper made on alloys with a range in thickness from  $20 \text{ \AA}$  to  $5 \times 10^4 \text{ \AA}$  were therefore designed for this purpose, and we now present an analysis of the data collected on 15 such specimens. The sputtered alloys were of nominal composition,  $\text{Cu}_{50}\text{Ti}_{50}$ —a system that has none of the complications of ferromagnetism or superconductivity.

## 2. Background analysis

There is now a lot of evidence supporting the idea of the importance of quantum corrections to the classical theory of electrical conduction in amorphous alloys and this has been the subject of several recent reviews (see, e.g., Alt'shuler and Aronov 1985, Bergmann 1984, Dugdale 1987, Howson and Gallagher 1988, Lee and Ramakrishnan 1985, Naugle 1984). A central feature is the concept of weak localization whereby electrical conduction is reduced by the interference between wavelets scattered by neighbouring atoms in the disordered alloy—an effect that is most extreme at very low temperatures. At higher temperatures the phase coherence of the scattered wavelets is destroyed by inelastic scattering, and so the conductivity rises with increasing  $T$ . However, because of the different integrals arising from summing over different dimensions, the forms of the temperature dependences for 3D and 2D specimens are completely different (see, e.g., Alt'shuler and Aronov 1985). For 3D materials the temperature-dependent component of conductivity,  $\Delta\sigma_{3D}(T)$ , is given by

$$\Delta\sigma_{3D}(T) \sim e^2/\pi^2 \hbar L_{\phi} \quad (1)$$

† Present address: Cavendish Laboratory, Madingley Road, Cambridge, UK.

where  $L_\varphi$ , the phase coherence length for inelastic or spin-flip scattering, is related to the scattering rate,  $\tau_\varphi^{-1}$ , by  $L_\varphi = (D\tau_\varphi)^{1/2}$  with  $D$  the diffusion constant of the alloy. Since only inelastic processes vary with temperature we have

$$\Delta\sigma_{3D} \propto T^{p/2} \quad (2)$$

where  $p$  is the index of the temperature dependence of the inelastic scattering rate according to  $\tau_\varphi^{-1} \propto T^p$ . As an example, we may consider the case of electron-electron scattering for which  $p = 2$ ; the form of equation (2) is then  $\Delta\sigma_{3D}(T) \propto T$ . For 2D specimens, on the other hand, the form of the expression is

$$\Delta\sigma_{2D} \propto (p/2) \ln(T/T_0). \quad (3)$$

It should be emphasized that although quantum corrections are normally subdivided into those involving the localization of single electrons and those involving electron correlations—that is, effects termed ‘localization’ and ‘interaction’, respectively—the form of these expressions is the same for both. Bergmann (1987) has explained the similarity by showing that while in the former two scattered waves interfere, in the latter the interference is between a scattered and a non-scattered electron. The relative importance of the two effects can be described by two scale lengths: a localization length

$$L_{\text{loc}} = (D\tau_i)^{1/2} \quad (4a)$$

and an electron coherence length

$$L_{\text{cc}} = (\hbar D/kT)^{1/2}. \quad (4b)$$

When  $L_{\text{loc}}$  and  $L_{\text{cc}}$  are both greater than  $t$ , the specimen thickness, the material is quasi-2D. We should also note in passing that for such disordered systems the *principal* scattering length—the elastic scattering length—is always extremely small, of the order of inter-atomic dimensions, and so the classical Fuchs and Sondheimer thin-film corrections can be neglected.

Although we have previously shown in detail the application of equation (2) to melt-spun Cu-Ti ribbons (Howson and Greig (1986); see also Schulte and Fritsch (1986)) and although there have been a number of reports of applying equation (3) to semiconducting thin films, such comparisons have never been made on the *same* disordered system in which thickness is the only variable parameter.

### 3. Experimental details

The specimens were made by sputtering in commercial Ion Tech equipment from a polycrystalline button of a Cu-Ti alloy of the required composition. During deposition the substrate temperature never exceeded 300 K which is well below the crystallization temperature of the 50:50 amorphous alloy. The chamber was initially evacuated by a cryopump to a background pressure of less than  $10^{-7}$  Torr with the residual components mainly water, helium and hydrocarbons. Careful tests were made to determine the optimum sputtering pressure of the ionized Ar gas, as using too high a pressure resulted in granular material that was quite unsatisfactory being produced. The conditions used in sputtering each of the 15 films is given in table 1.

The sputtering cycles were always preceded by cleaning the soda-glass substrates by a fast-atom source for about three minutes followed by sputtering the film to the required thickness. Finally, masks were interchanged so that a series of copper bars about  $0.5 \mu\text{m}$  thick were deposited on top of the specimen, to act as current and voltage probes. Film thicknesses greater than  $0.1 \mu\text{m}$  could be measured directly with a Dektak stylus to an

**Table 1.** Details of specimens: argon pressure,  $P_s$ , and sputtering time,  $T_s$ , for specimens of thickness,  $t$ , and room temperature resistance,  $R$ . The characteristic temperature,  $T_x$ , and the factor  $\alpha p + \beta$  are explained in the text. From an average value of resistivity of  $230 \mu\Omega \text{ cm}$  we deduce that the *elastic* mean free path in these alloys is only about  $3.4 \text{ \AA}$ .

Specimen	$t$ ( $\text{\AA}$ )	$P_s$ (mTorr)	$T_s$ (s)	$R$ ( $\Omega$ )	$T_x$ (K)	$\alpha p + \beta$
I	20	7.1	37	2800	10.0	1.14
II	30	6.9	56	977	6.0	0.54
III	40	6.8	74	466	5.7	0.30
IV	50	7.1	93	697	4.7	0.75
V	100	7.3	60	648	5.5	1.22
VI	100	7.3	60	648	—	—
VII	100	7.4	60	771	—	—
VIII	300	7.4	165	179	4.5	0.95
IX	500	7.2	270	107	4.5	1.46
X	700	8.4	375	60.2	4.5	1.20
XI	1000	8.4	510	50.6	—	—
XII	10000	7.0	5400	4.30	—	—
XIII	10000	7.0	5400	5.27	—	—
XIV	10000	7.1	5400	5.17	—	—
XV	50000	8.4	26400	1.04	—	—
XVI	420000	Melt-spun				

accuracy of about 10%. These results were then used to calibrate the sputterer so that the thickness of the thinnest films could be deduced from details of the sputtering power and time. The thicker films were shown to be amorphous by x-ray diffraction, while a selection of specimens examined by TEM were, without exception, found to be crack-free and continuous.

The transport properties were measured by a conventional four-probe DC method in a specially constructed top-loading cryostat fitted with a 7 T superconducting magnet, and with a sample stage designed so that specimens could sit either parallel or perpendicular to the magnetic field. Complete control of the measuring processes and temperature stability of the cryostat to better than 10 mK were achieved using an IBM PC interfaced to several Keithley 181 nanovoltmeters.

#### 4. Results and discussion

As the films were all of the same 50:50 composition and were made with approximately the same geometry, we expect that the resistance should be inversely proportional to thickness, and this is confirmed in figure 1. The resistivity,  $\rho$ , is therefore independent of thickness and from the data we have deduced an average value of  $230 \pm 20 \mu\Omega \text{ cm}$ . This is in agreement with several other studies of vapour-quenched alloys, although—also in accordance with earlier studies—the measurements are about 20% higher than the resistivity of melt-spun ribbons. For example, whereas values of  $186 \mu\Omega \text{ cm}$  (Mizutani *et al* 1983),  $192 \mu\Omega \text{ cm}$  (Howson and Greig 1984), and  $195 \mu\Omega \text{ cm}$  (Howson 1984) have been reported for melt-spun ribbons, previous measurements on sputtered/vapour-deposited films have given resistivities of  $260 \mu\Omega \text{ cm}$  (Drewery and Friend 1987) and  $250 \mu\Omega \text{ cm}$  (Rathnayaka *et al* 1986). Similar differences have been noted in other amorphous alloy systems, probably as a consequence of the greater degree of disorder

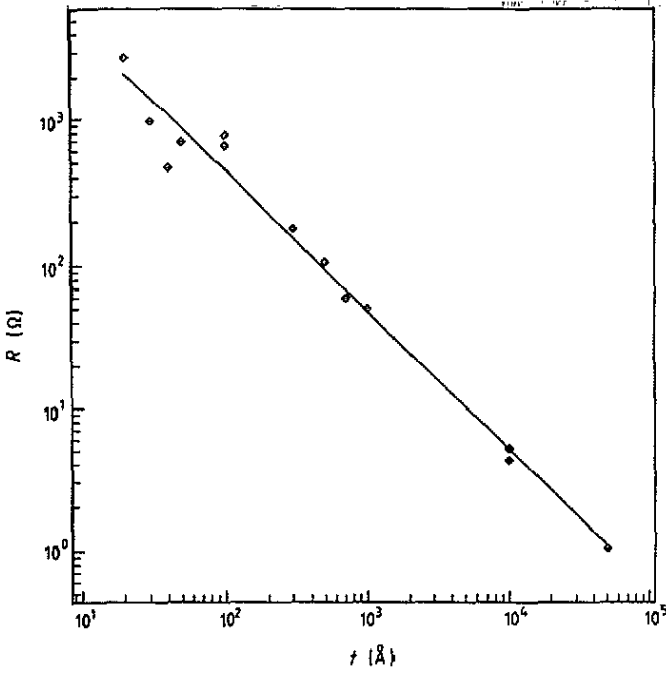


Figure 1. Variation of room temperature resistance,  $R$ , with film thickness,  $t$ , for the specimens listed in table 1. The line is a least-squares fit of slope  $0.97 \pm 0.2$ .

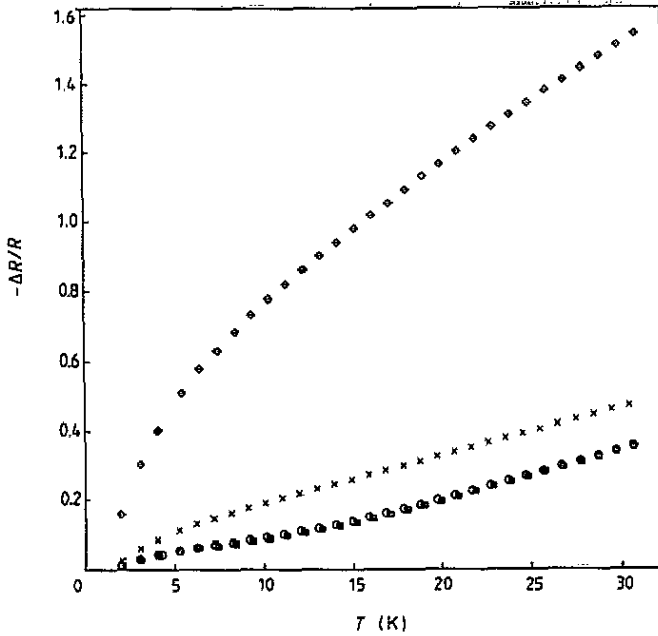
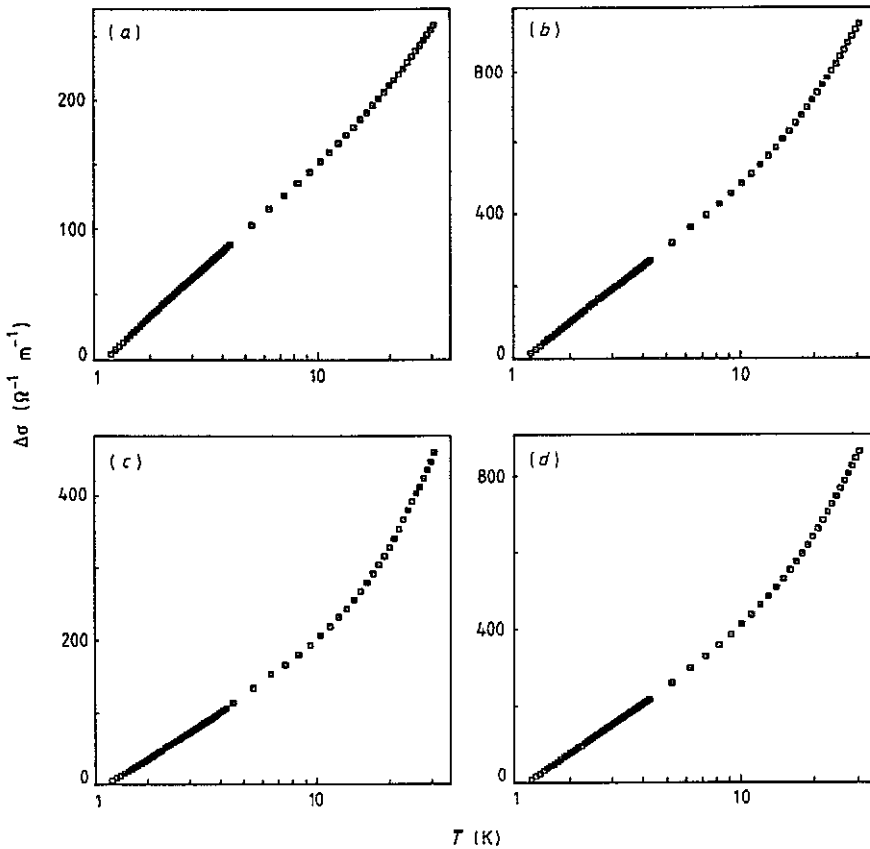


Figure 2. Percentage change in resistance with temperature for films of thickness 100 Å ( $\diamond$ ), 1000 Å ( $\times$ ), 5  $\mu\text{m}$  ( $\circ$ ) together with data from a 42  $\mu\text{m}$  melt-spun alloy ( $\square$ ) of the same nominal composition.



**Figure 3.** Temperature-dependent component of conductivity  $\Delta\sigma = \sigma(T) - \sigma(1.3)$  as a function of  $\ln T$  for films of thickness (a) 20 Å, (b) 30 Å, (c) 40 Å and (d) 50 Å.

in sputtered or vapour-deposited specimens. Nevertheless, although the absolute values of resistivity show this marked difference between sputtered and melt-spun alloys we found that the differences in the temperature and field dependences—that is the differences in the properties central to this paper—were absolutely negligible.

This is clearly illustrated in figure 2 where we show the fractional change of resistance  $-\Delta R/R$  with temperature for a selection of the films and a melt-spun alloy of the same nominal composition. We see that although  $\Delta R/R$  is strongly dependent on thickness, for the thickest alloys the method of preparation is immaterial. The much greater fractional change in the thinnest specimen is a general feature of quantum corrections, and is reflected in the form of equation (1).

In figures 3 and 4 we show this temperature dependence in more detail for all specimens thinner than 1000 Å, this time plotting the change of conductivity with  $\ln T$  in order to make a more detailed comparison with equation (3). It is clear that below some characteristic temperature,  $T_x$ ,  $\Delta\sigma/\sigma$  is directly proportional to  $\log T$  where  $T_x$  varies from about 10 K in the thinnest specimens to about 4.5 K in the thickest (table 1). It is therefore apparent that at low enough temperatures all these specimens exhibit 2D behaviour, but that there is a departure from this when the thickness becomes greater than either of the scale lengths  $L_{loc}$  or  $L_{ec}$ . Our estimates based on equation (4) show that  $L_{ec}$  evaluated as  $T_x$  is always less than 100 Å, while  $L_{loc}$ , deduced from magnetoresistance

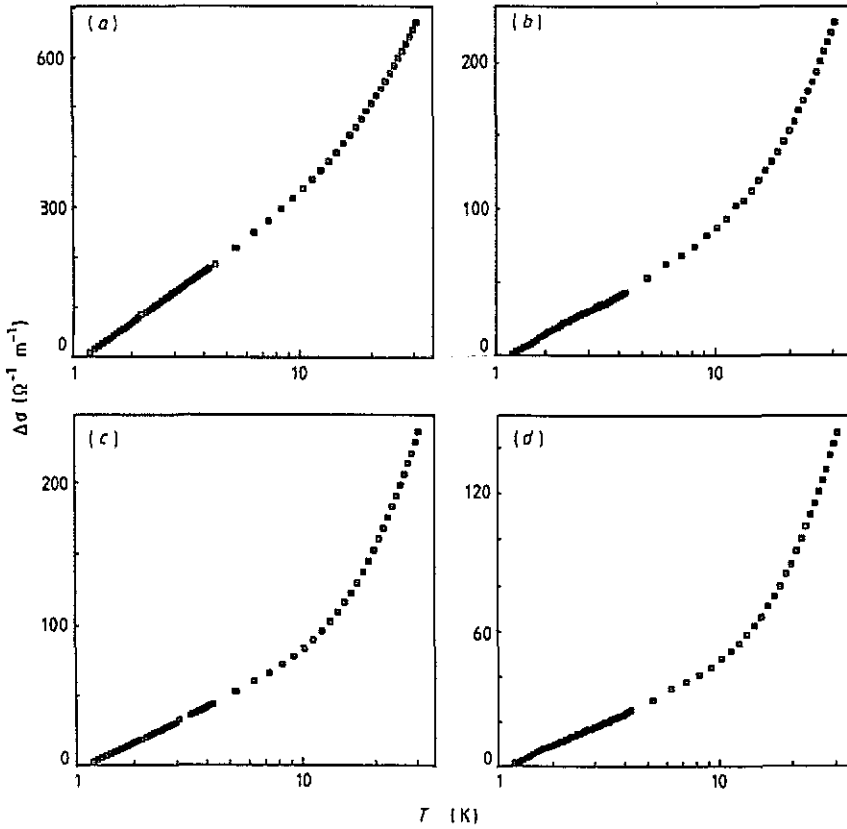


Figure 4. Temperature-dependent component of conductivity  $\Delta\sigma = \sigma(T) - \sigma(1.3)$  as a function of  $\ln T$  for films of thickness (a) 100 Å, (b) 300 Å, (c) 500 Å and (d) 700 Å.

measurements (see Hickey *et al* 1987), is considerably greater than the sample thickness in all specimens included in figures 3 and 4. We conclude that the departure from  $\ln T$  in these specimens is therefore due to a change in dimension as determined by the effects of interaction. Above  $T_x$  the temperature dependence therefore arises from the combined effects of 3D interaction and 2D localization making a detailed analysis significantly more difficult, and the purpose of this short paper is to emphasize the much simpler regime at the lowest temperatures.

Examining the temperature dependence of the thinnest samples in more detail we see from equation (3) that  $p$ , the index of the temperature dependence of the inelastic scattering rate, can be easily obtained from the variation of  $\Delta\sigma(T)$  with  $\ln T$ . For 3D ribbons reported values of  $p$  have varied between 1 and 4 depending on the predominant scattering mechanism, although it is clear that the simple power law,  $\tau_1 \propto T^p$ , is often inadequate (Belitz and Das Sarma 1987, Hickey *et al* 1987). In particular the effects of spin-orbit, magnetic and many-body (interaction) effects greatly complicate the theory, and an all-embracing form of equation (3) is

$$\Delta R_{\square}(T)/R_{\square} = -(e^2/2\pi^2\hbar)(\rho/t)(\alpha p + \beta) \ln(T/T_0) \quad (5)$$

where  $R_{\square} = \rho/t$ , the resistance per square of a sample of resistivity and thickness  $t$ , and where  $\alpha$  and  $\beta$  are the magnetic and many-body factors respectively (see Alt'shuler and Aronov 1985). For strong spin-orbit scattering  $\alpha = -\frac{1}{2}$ , for weak spin-orbit scattering

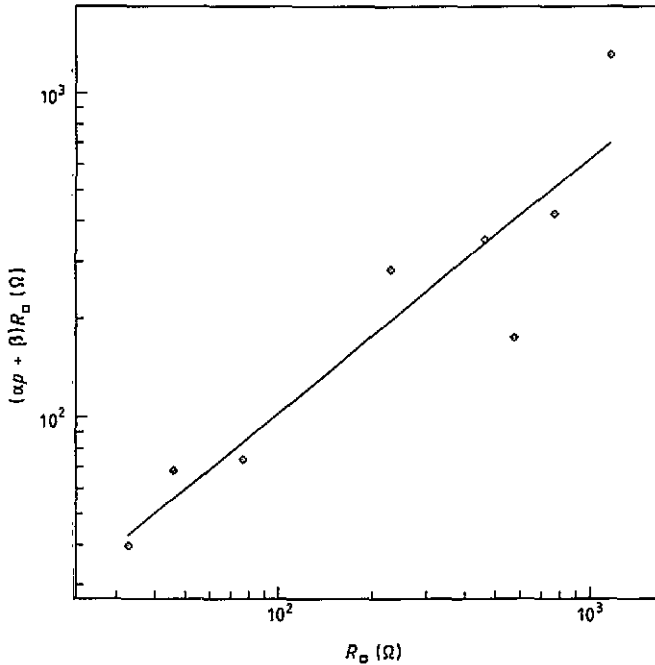


Figure 5. Variation of  $(\alpha p + \beta)R_{\square}$  with  $R_{\square}$  deduced from the low-temperature data in figures 3 and 4. The line is a least-squares fit giving  $\alpha p + \beta = 0.4 \pm 0.2$ .

$\alpha = 1$ , while for magnetic scattering  $\alpha = 0$  (Hikami *et al* 1980). The other parameter  $\beta$  is related to the screening factor,  $F$ , and the electron-phonon enhancement factor,  $\lambda$ , by  $\beta = 1 - (3/4)(F - \lambda)$ .

In figure 5 we show the experimental variation of  $(\alpha p + \beta)R_{\square}$  with  $R_{\square}$  from the low-temperature data on the thinnest specimens. Apart from measurements on the 20 Å sample for which we suspect the film is not continuous, the experimental value of  $\alpha p + \beta$  is  $0.4 \pm 0.2$ . As  $F$  and  $\lambda$  are both small factors  $\approx 0.3$  and therefore tend to cancel (see, e.g., Hickey *et al* 1987) it is clear that  $\beta$  must be approximately equal to 1 and that  $\alpha p$  must therefore be *negative*. This in turn indicates the presence of strong spin-orbit scattering—a factor entirely in keeping with the positive magnetoresistance and with previous evidence that spin-orbit scattering is greatly enhanced at surfaces (Lindelof and Wang 1986, Van Haesendonck *et al* 1985, Vranken *et al* 1988). In the present instance these surfaces are represented by the presence of grain boundaries observed as small metallic regions in the electron micrographs.

Finally as further evidence of 2D behaviour we draw attention to the very marked anisotropy of magnetoresistance in the thinner specimens. In our earlier studies of electron transport in amorphous alloys (see, e.g., Howson and Greig 1986) we noted that although the magnetoresistance at low temperatures is many orders of magnitude greater than predicted by free-electron models, nevertheless it is always isotropic. In figure 6 we show clear confirmation of this point by showing the magnetoresistance both parallel and perpendicular to the surface of a 1000 Å film at five different temperatures. For a 100 Å film, on the other hand, the results are completely different, and in figure 7 we show the striking anisotropy in such a specimen. The detailed study of magnetoresistance gives further insight into this whole problem and will in itself make an interesting area for future study.



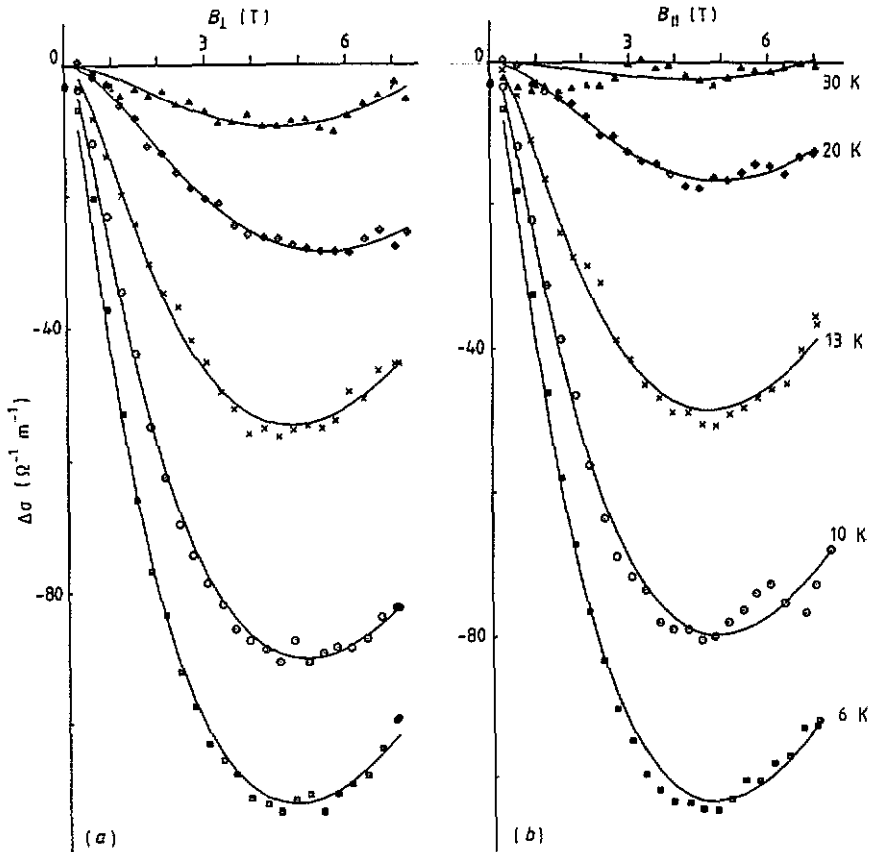


Figure 6. Absence of anisotropy in the magnetoconductivity  $\Delta\sigma = \sigma(B) - \sigma(0)$  of a 1000 Å film at five different temperatures, for (a)  $B$  perpendicular and (b)  $B$  parallel to the film surface. The curves are theoretical fits used in estimating  $\tau$ .

## 5. Summary

The measurements provide further evidence of the relevance of weak localization and electron-electron interaction in highly disordered alloys by showing a  $\ln T$  variation in the temperature dependence of the electrical conductivity in the thinnest specimens. For all such quasi-2D materials of thickness less than 1000 Å this  $\ln T$  dependence is observed below some characteristic temperature  $T_x$ . We have interpreted  $T_x$  as the temperature below which both the localization length and the electron-electron coherence length are greater than the specimen's thickness. Values of the slope of the linear portion of the  $\log T$  curves indicate the presence of strong spin-orbit scattering which we speculate might be at the surfaces or grain boundaries in the specimens.

## Acknowledgments

We should like to express our sincere thanks to the SERC and the Henry Ellison Scholarship fund of the University of Leeds for financial support, to A A M Croxon, M Simpson and M J Walker for their considerable help in the experimental programme,

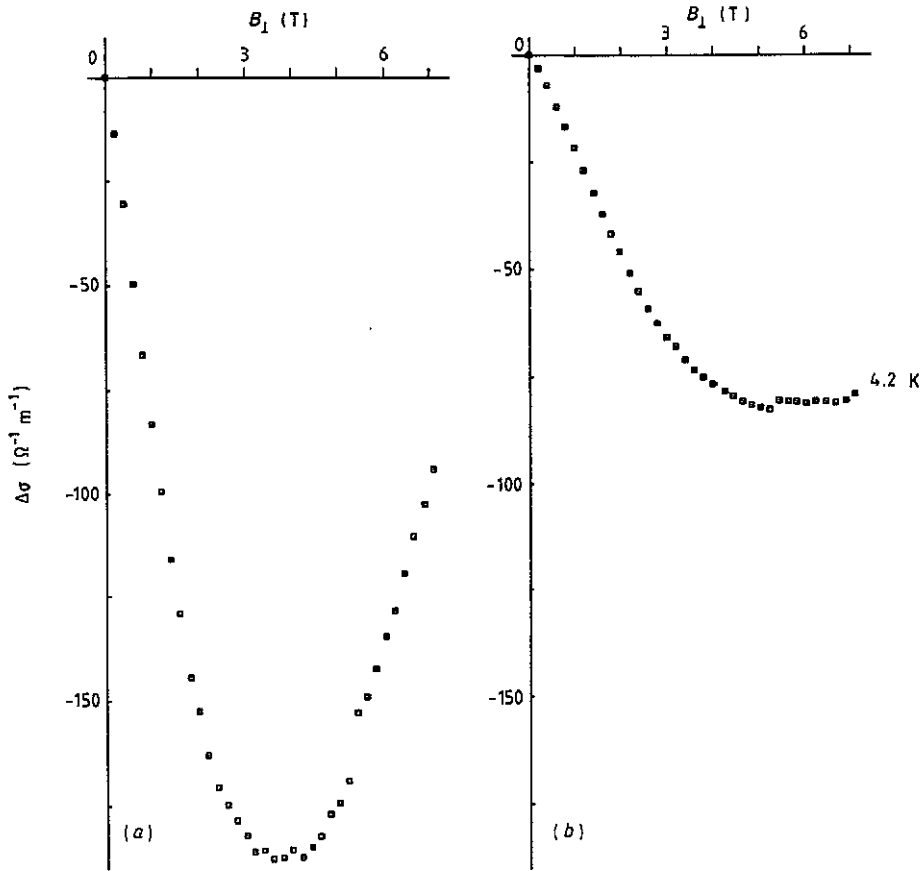


Figure 7. Anisotropy in the magnetoconductivity of a 100 Å film at 4.2 K for (a)  $B$  perpendicular and (b)  $B$  parallel to the film surface.

and to B J Hickey, M A Howson and G J Morgan for many discussions on the subject of localization and interaction in amorphous metallic alloys.

## References

- Alt'shuler B L and Aronov A G 1985 *Electron-Electron Interactions in Disordered Systems* ed A L Efros and M Pollak (Amsterdam: Elsevier Science)
- Belitz D and Das Sarma S 1987 *Phys. Rev. B* **36** 7701
- Bergmann G 1984 *Phys. Rep.* **107** 1
- 1987 *Phys. Rev. B* **35** 4205
- Drewery J S and Friend R H 1987 *J. Phys. F: Met. Phys.* **17** 1739
- Dugdale J S 1987 *Contemp. Phys.* **28** 547
- Hickey B J, Greig D and Howson M A 1987 *Phys. Rev. B* **36** 3074
- Hikami S, Larkin A I and Nagaoka Y 1980 *Prog. Theor. Phys.* **63** 707
- Howson M A 1984 *J. Phys. F: Met. Phys.* **14** L25
- Howson M A and Gallagher B L 1988 *Phys. Rep.* **170** 265
- Howson M A and Greig D 1984 *Phys. Rev. B* **30** 4805
- 1986 *J. Phys. F: Met. Phys.* **16** 989

- Lee P A and Ramakrishnan T V 1985 *Rev. Mod. Phys.* **57** 287  
Lindelof P E and Wang S 1986 *Phys. Rev. B* **33** 1478  
Mizutani U, Akutsu N and Mizoguchi T 1983 *J. Phys. F: Met. Phys.* **13** 2127  
Naugle D G 1984 *J. Phys. Chem. Solids* **45** 367  
Rathnayaka K D D, Kaiser A B and Trodahl H J 1986 *Phys. Rev. B* **33** 889  
Schulte A and Fritsch G 1986 *J. Phys. F: Met. Phys.* **16** L55  
Van Haesendonck, Gijs M and Bruynseraede Y 1985 *Localization, Interaction and Transport Phenomena* ed B Kramer, G Bergmann and Y Bruynseraede (Berlin: Springer)  
Vranken J, Van Haesendonck C and Bruynseraede Y 1988 *Phys. Rev. B* **37** 8502